● Original Paper ●

Atmospheric Precursors of and Response to Anomalous Arctic Sea Ice in CMIP5 Models

Michael KELLEHER and James SCREEN*

College of Engineering, Mathematics and Physical Sciences, University of Exeter, Exeter EX4 4QE, UK

ABSTRACT

This study examines pre-industrial control simulations from CMIP5 climate models in an effort to better understand the complex relationships between Arctic sea ice and the stratosphere, and between Arctic sea ice and cold winter temperatures over Eurasia. We present normalized regressions of Arctic sea-ice area against several atmospheric variables at extended lead and lag times. Statistically significant regressions are found at leads and lags, suggesting both atmospheric precursors of, and responses to, low sea ice; but generally, the regressions are stronger when the atmosphere leads sea ice, including a weaker polar stratospheric vortex indicated by positive polar cap height anomalies. Significant positive midlatitude eddy heat flux anomalies are also found to precede low sea ice. We argue that low sea ice and raised polar cap height are both a response to this enhanced midlatitude eddy heat flux. The so-called "warm Arctic, cold continents" anomaly pattern is present one to two months before low sea ice, but is absent in the months following low sea ice, suggesting that the Eurasian cooling and low sea ice are driven by similar processes. Lastly, our results suggest a dependence on the geographic region of low sea ice, with low Barents–Kara Sea ice correlated with a weakened polar stratospheric vortex, whilst low Sea of Okhotsk ice is correlated with a strengthened polar vortex. Overall, the results support a notion that the sea ice, polar stratospheric vortex and Eurasian surface temperatures collectively respond to large-scale changes in tropospheric circulation.

Key words: sea ice–atmosphere coupling, stratosphere–troposphere coupling, atmospheric circulation, Eurasian climate

Citation: Kelleher, M., and J. Screen, 2018: Atmospheric precursors of and response to anomalous Arctic sea ice in CMIP5 models. *Adv. Atmos. Sci.*, **35**(1), 27–37, https://doi.org/10.1007/s00376-017-7039-9.

---

1. Introduction

Changes in Arctic sea ice have a direct impact on the local atmosphere and ocean in the region of ice loss; however, the remote impacts of changing sea ice are less well understood. As ice is lost, open ocean with lower albedo is exposed, giving rise to increased surface heat and moisture fluxes from the ocean into the atmosphere. This is hypothesized to weaken the equator-to-pole temperature gradient, thereby having an impact on midlatitude circulation. Multiple review papers, including Cohen et al. (2014), Vihma (2014), Walsh (2014) and Overland et al. (2016), have assembled the current status of our understanding of the interactions between Arctic sea ice and the atmosphere, both locally and remotely. Overland et al. (2016) suggested a nonlinear dependence on the state of the atmosphere–ocean–sea-ice system that means not all changes in sea ice lead to the same atmospheric response. It should also be noted that while connections between Arctic and midlatitude weather have been demonstrated, the inter-annual variability is affected by many other factors, including sea surface temperatures and tropical teleconnections.

The atmospheric geopotential height over the polar cap can be used to identify changes in circulation, and is strongly related to the mean temperature below a particular level. Changes in temperatures at lower levels can impact the atmosphere above through this relationship. The work by Sun et al. (2015) showed that changes in sea ice can impact the mid-to-upper tropospheric and lower stratospheric circulation in an idealized model. This is supported by the results of Peings and Magnusdottir (2014), Kim et al. (2014) and Nakamura et al. (2016), among others, who identified a connection with the stratosphere. However, such studies were largely concerned with the response to low sea ice and did not explicitly consider the causes of low sea ice in the first instance. In the present study, we suggest that the atmospheric conditions that precede low sea ice can also weaken the polar stratospheric vortex directly.

There is an established relationship between mid-tropospheric eddy meridional heat flux, which is the vertical component of Eliassen–Palm wave activity flux (Edmon et al., 1980), and stratospheric circulation (e.g., Newman and Nash, 2000; Sjoberg and Birner, 2012). Enhanced heat flux, or upward wave activity relative to climatology, over a pe-

---

* Corresponding author: James SCREEN
  Email: j.screen@exeter.ac.uk

riod of a few months has been shown to be related to a weakened stratospheric polar vortex. Thereafter, changes in polar stratospheric circulation have been shown to enhance long time scale predictability in the troposphere (Baldwin and Dunkerton, 2001; Christiansen, 2001; Baldwin et al., 2003). As enhanced tropospheric meridional heat flux affects the stratosphere, and is also associated with midlatitude circulation anomalies that may affect sea ice, we speculate that midlatitude circulation anomalies associated with positive eddy heat flux anomalies can affect both Arctic sea ice and the stratospheric circulation directly, and then provide evidence for this speculation. This complicates the assessment of causality of sea-ice–stratosphere linkages, as both may be responding to eddy heat flux anomalies rather than the sea ice driving the stratosphere directly.

A hypothesized impact of Arctic sea ice loss is the "warm Arctic, cold continent" pattern in surface temperatures. Work by Mori et al. (2014) suggested that more frequent Eurasian blocking due to sea ice loss forces cold-air advection into the region and thus cooler Eurasian winters. In Petoukhov and Semenov (2010) a similar process was discussed, though the resulting pattern was found to be nonlinearly dependent on the degree of sea ice loss. The work of McCusker et al. (2016) and Sun et al. (2016), however, provided modelling evidence that while a warm Arctic is driven by sea ice loss, the cold continental temperature pattern may not be. Sorokina et al. (2016) found a robust relationship between turbulent heat flux and Barents–Kara Sea ice using reanalysis data, though the link to cold continental temperatures was not apparent. As the "warm Arctic, cold continent" is a pattern that can be driven purely by internal variability, we attempt, by means of lead–lag regressions, to elucidate its temporal evolution and infer the directionality of the relationship between this pattern and Arctic sea ice.

The atmospheric response to sea ice loss is likely to be sensitive to the geographical location of the ice anomalies. The results of Petoukhov and Semenov (2010), Sun et al. (2015), Koenigk et al. (2016), Pedersen et al. (2016), Screen (2017b) and others suggest that different regions of ice loss have different response patterns. This is possibly related to the interference with the climatological mean planetary wave (Martius et al., 2009; Garfinkel et al., 2010; Smith et al., 2011), whereby constructive (destructive) interference between the forced and climatological planetary waves acts to enhance (suppress) vertical wave propagation. For this reason, the present study examines relationships with pan-Arctic anomalies as well as with regional sea ice anomalies.

This paper seeks to further our understanding of the precursors of, and response to, Arctic sea ice loss, presenting evidence from CMIP5 climate models. The CMIP5 models have been a relatively underused resource in this regard, with the notable exception of Boland et al. (2017). In contrast to Boland et al. (2017), who examined historical and future scenarios, we focus on pre-industrial control simulations to examine the internal variability in the absence of forced trends. We are especially motivated to better understand the nature of the coupled two-way relationship between Arctic sea ice

and the stratospheric polar vortex, and additionally between Arctic sea ice and cold winter temperatures over Eurasia, as present within the selected CMIP5 models.

2. Data and methods

The data used in this study are from the CMIP5 archive. Monthly means from the pre-industrial control simulations are used, as the purpose of the investigation is to examine relationships between sea ice and the atmosphere that occur as part of the natural climate variability. There are 34 models (Table 1) that have the required data available. We first examine this group as a whole, before then using a subset of models with different model genealogy (Knutti et al., 2013), which can be considered to be roughly independent of one another. The model subset is denoted with bold text in Table 1, and is selected such that one model per family is chosen and, where possible, similar horizontal resolutions are used. The

Table 1. Details of the models with sufficient availability of sea ice and atmospheric data. Models in bold text are those used in the primary subset, while those marked with an asterisk are the ones used in the high-top subset. Further details on these models are available in http://cmip-pcmdi.llnl.gov/cmip5/.

Model	Lat × Lon	Model top (hPa)	Years
ACCESS1.0	145 × 192	10	499
ACCESS1.3	145 × 192	10	499
BCC_CSM1.1	64 × 128	2.917	499
BCC_CSM1.1(m)	160 × 320	2.917	399
BNU-ESM	64 × 128	2.194	558
CCSM4	192 × 288	2.194	1050
CESM1(BGC)	192 × 288	2.194	499
CESM1(CAM5)	192 × 288	2.194	318
CESM1(FASTCHEM)	192 × 288	2.194	221
CESM1(WACCM)*	96 × 144	5.1	199
CMCC-CESM	48 × 96	0.01	276
CMCC-CM	240 × 480	10	329
CMCC-CMS	96 × 192	0.01	499
CNRM-CM5	128 × 256	10	849
FGOALS-g2	64 × 128	2.194	699
FGOALS-s2	108 × 128	2.19	500
GFDL CM3*	90 × 144	0.01	499
GFDL-ESM2G	90 × 144	3.65	499
GFDL-ESM2M	90 × 144	3.65	499
HadGEM2-CC*	145 × 192	0.04	240
INM-CM4.0	46 × 240	0.1	499
IPSL-CM5A-LR	96 × 95	0.04	999
IPSL-CM5A-MR*	144 × 143	0.04	299
IPSL-CM5B-LR	96 × 95	0.04	299
MIROC-ESM	64 × 128	0.003	629
MIROC-ESM-CHEM	64 × 128	0.003	254
MIROC4h*	160 × 640	0.9	99
MIROC5	64 × 256	2.9	699
MPI-ESM-LR	96 × 192	0.01	999
MPI-ESM-MR*	96 × 192	0.01	999
MPI-ESM-P	96 × 192	0.01	1155
MRI-CGCM3*	320 × 160	0.01	499
NorESM1-M	48 × 144	2.194	500
NorESM1-ME	48 × 144	2.194	251

results from this subset of models are qualitatively similar to those using the full set of models; however, there are quantitative differences in the magnitude of the regressions and their statistical significance. We argue that the non-independence of the models in the full set leads to overconfidence and, therefore, opt to use the smaller set of independent models here. Selected results from a similarly constructed set of high-top models are also presented. These demonstrate that the specific selection of models does not impact the results qualitatively.

Time series of isobaric geopotential height and sea ice area (sea ice concentration multiplied by grid cell area) over the polar cap (66°–90°N), and zonal-mean meridional eddy heat flux ($\overline{v'T'}$) over 45°–65°N are calculated. This latitudinal band for the averaging of heat flux is different to that used in previous studies (e.g., Newman and Nash, 2000; Sjoberg and Birner, 2012) in order to separate the Arctic and midlatitudes, but this choice does not affect the results qualitatively. The time series of each variable is then used to calculate standardized climatological anomalies, $x' = (\bar{x} - x)/s_x$, where $\bar{x}$ and s_x are the long-term monthly mean and standard deviation for the nearest 30 years to the modelled monthly variable x.

The standardized sea ice area anomalies are regressed against the diagnostic variable anomalies at leads and lags of up to 14 months. To generate seasonal regressions, sea ice is masked such that only anomalies from each individual season are regressed against the atmospheric variables of all seasons. This means a lag of −3 in the December–

January–February (DJF) mean is a mean of the regression of all December sea ice with September diagnostic variables, January sea ice with October diagnostic variables, and February sea ice with November diagnostic variables. In all plots, we show the negative regression slope, as this enables the association between the atmosphere and low sea ice conditions to be demonstrated. Statistical significance is calculated using Fisher's method (Kost and McDermott, 2002).

3. Results

3.1. *Polar cap height*

We begin by looking at the linear regression between sea ice area and polar cap height at extended lead and lag times (Fig. 1) for the set of all CMIP5 models with data available. There are statistically significant regressions at both positive and negative lags, implying both atmospheric precursors of, and responses to, low sea ice. Positive (anticyclonic) anomalies are the dominant signal through most of the atmosphere, with significant anomalies at both positive and negative lag times. This indicates that low sea ice is preceded by, and followed by, tropospheric high geopotential height anomalies in the Arctic region. In general, the regressions are stronger when the atmosphere leads sea ice, which suggests that sea ice, at least initially, is not forcing the changes in the polar mid-to-upper troposphere and lower stratosphere. This is especially the case for low summer and low autumn sea ice, suggesting sea ice in these seasons is particularly sensitive to
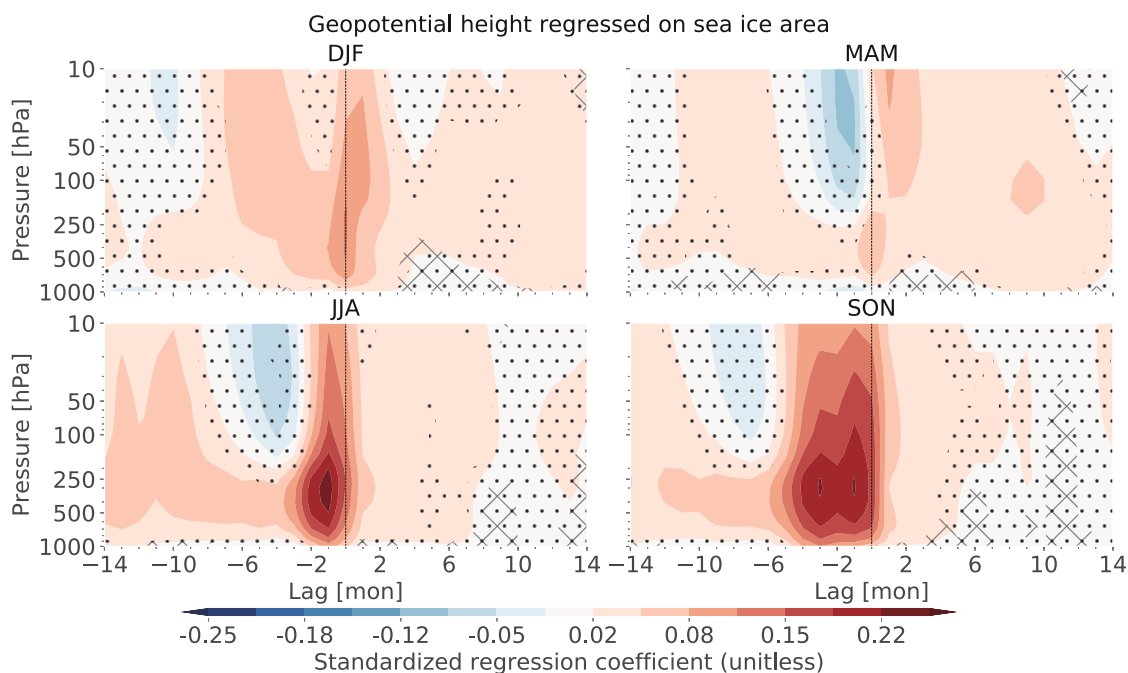

Geopotential height regressed on sea ice area

Fig. 1. Linear regression of standardized polar cap sea ice area anomalies against standardized polar cap geopotential height anomalies for each season for the full set of models. The regressions have been multiplied by minus one to show the patterns associated with low sea ice. Hatching covers areas not statistically significant at the 99% confidence level, while dots cover areas where fewer than 75% of models agree with the sign of the regression slope. Negative lags indicate atmosphere leading sea ice. The shading is unitless (standardized regression coefficient).

the atmospheric conditions in preceding months. However, there are statistically significant positive anomalies in polar cap height following low sea ice in all seasons, but especially in winter and spring, which suggests a weakening of the polar stratospheric vortex following low sea ice.

Figure 2 is constructed in a similar manner to Fig. 1, but for the subset of independent models described in Table 1. There are some small but notable differences in the magnitude of the regressions (between the subset and full set), but the largest differences are in the areas of model agreement and statistical significance. Figure 3, showing the results from a subset of high-top (greater than 0.01 hPa) models, is similar to the previous two figures, with some key exceptions. The magnitudes of the regression slopes are higher, and all seasons show a statistically significant but weak negative anomaly in the early spring stratosphere. The latter may indicate a more persistent polar stratospheric vortex in spring, relative to the climatological mean transition to anticyclonic summer circulation. This could be a delay in the final stratospheric warming, the transition between winter (cyclonic) and summer (anticyclonic) stratospheric circulations, typically occurring in April. In general, the qualitative differences in the regressions are small (comparing the high-top subset and the full set), but the high-top subset has a smaller area of statistical significance and robustness compared to the full set. In the following figures, we show results only from the models of the first subset of independent models, as the differences between the two subsets and the full set are small. It should also be noted that the maximum regression slopes, as well as correlation coefficients, are small (maximums of 0.3), despite the relationship being robust across models and statistically significant. This is to be expected, as multiple factors influence atmospheric circulation in addition to sea ice.

3.2. *Eddy heat flux*

We now turn our attention to the midlatitude tropospheric meridional eddy heat flux (hereafter, "heat flux"), which is known to drive stratospheric variability and is the vertical component of the Eliassen–Palm flux. In all seasons, a statistically significant heat flux is found to precede anomalously low polar cap sea ice (Fig. 4). Enhanced heat flux is apparent in the lower troposphere for up to 6 months prior to low sea ice in winter and spring, and 12 months prior to low sea ice in summer and autumn. This strongly suggests that enhanced poleward heat flux contributes to the low sea ice anomalies. There is little evidence for the opposite—sea ice causing a change in the heat flux—with mostly insignificant regressions at positive lag times (i.e., following anomalously low ice). A positive heat flux is known to contribute to stratospheric polar vortex weakening. The heat flux anomalies preceding low sea ice are one likely cause of the enhanced polar cap height that also precedes low sea ice. Therefore, it is probable that the sea ice and polar cap height are both responding to this enhanced midlatitude heat flux—similar to the results of Perlwitz et al. (2015) and Screen et al. (2012) with respect to Arctic warming being driven by heat transport into the Arctic from lower latitudes.

3.3. *Surface temperature*

In previous work, low sea ice (and in some cases a weakened stratospheric polar vortex) has been proposed to cause the "warm Arctic, cold continent" winter temperature anomaly pattern. It has been argued that low Arctic sea ice
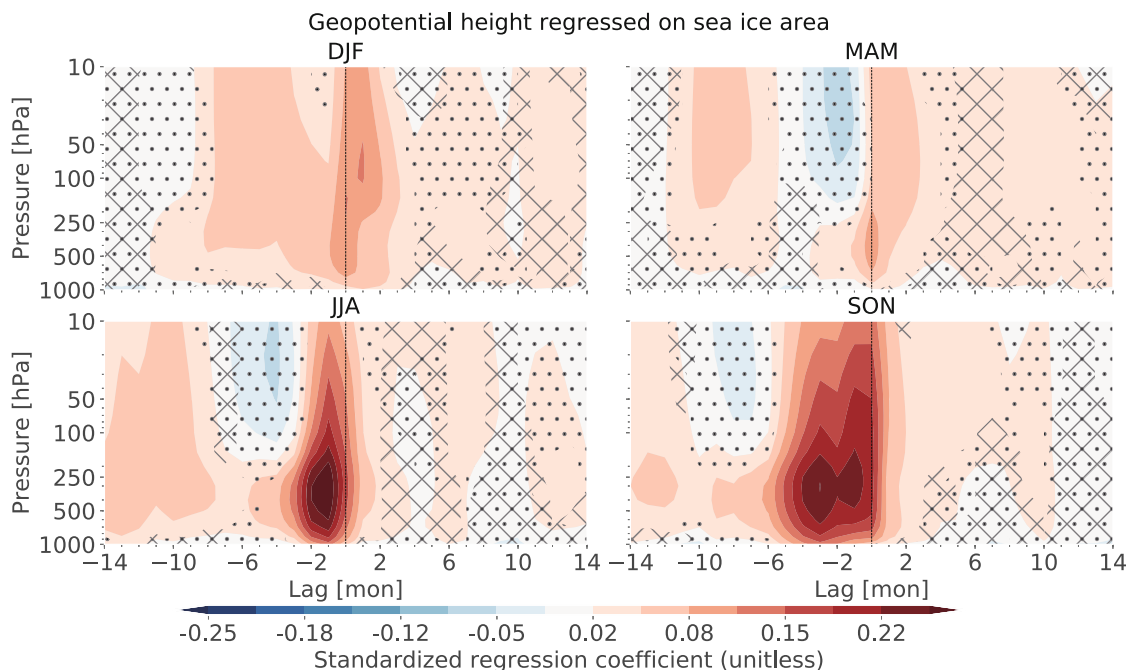

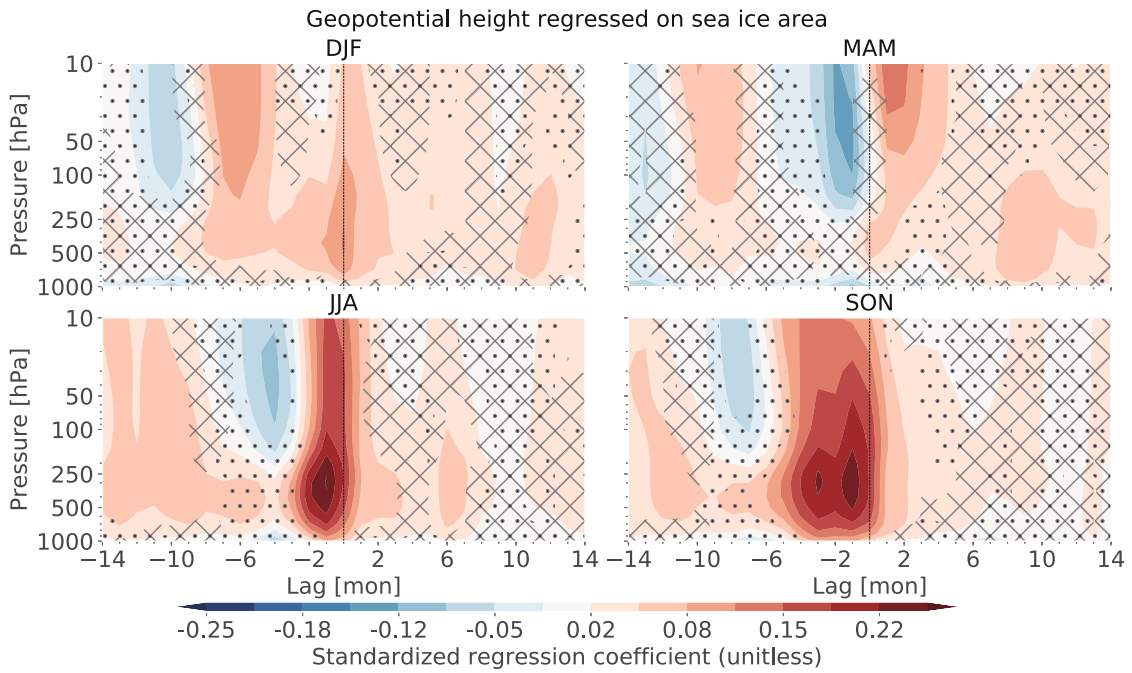**Fig. 2.** As in Fig. 1, but for the subset of eight selected models shown in Table 1.

Geopotential height regressed on sea ice area

Fig. 3. As in Fig. 1, but for the subset of six selected high-top models shown in Table 1.

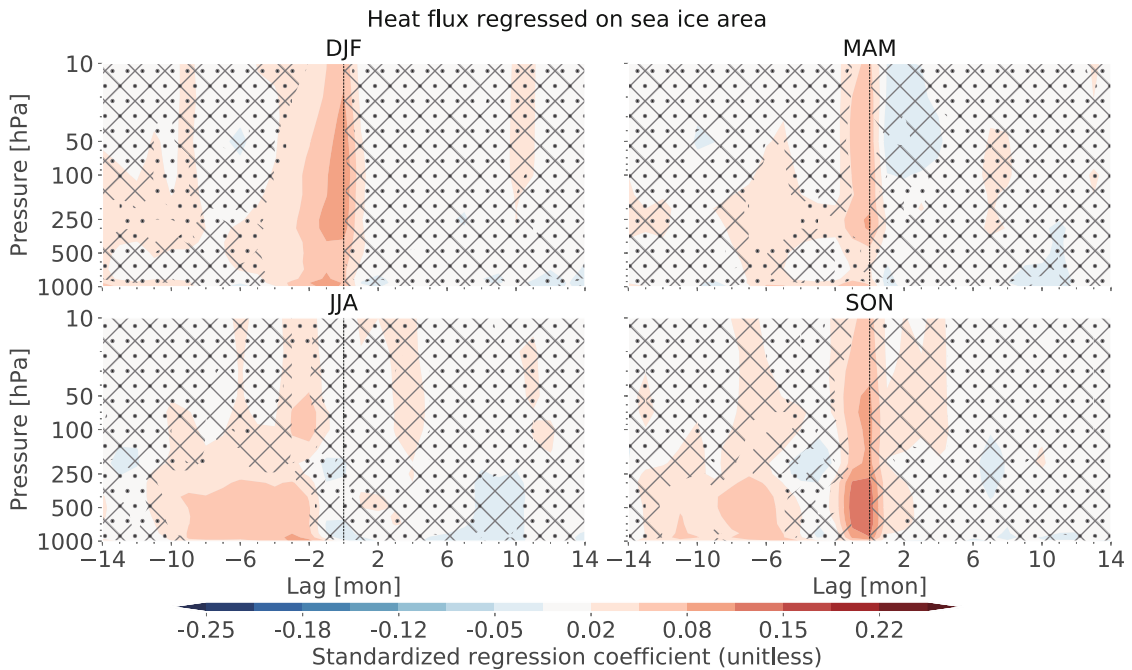Heat flux regressed on sea ice area

Fig. 4. As in Fig. 2 but for midlatitude meridional eddy heat flux standardized anomalies. The shading is unitless (standardized regression coefficient).

causes warmer Arctic surface temperatures but cooler conditions over Eurasia and North America (Honda et al., 2009; Petoukhov and Semenov, 2010; Cohen et al., 2013; Mori et al., 2014; Kug et al., 2015). Figure 5 shows the lead–lag relationship between winter sea ice and Northern Hemisphere surface temperature. The CMIP5 models reproduce the "warm Arctic, cold continent" anomaly pattern at zero lag, with significant cold winter temperature anomalies over

Eurasia correlated with low winter sea ice. This temperature anomaly pattern is also seen at a lag of −1 month and, to a lesser extent, at a lag of −2 months. This implies that both the Arctic warming and Eurasian cooling precede low winter sea ice.

The warm anomaly in the Arctic is maximized over the Barents–Kara Sea and is present for at least two months before low winter sea ice. The progression of anomalously
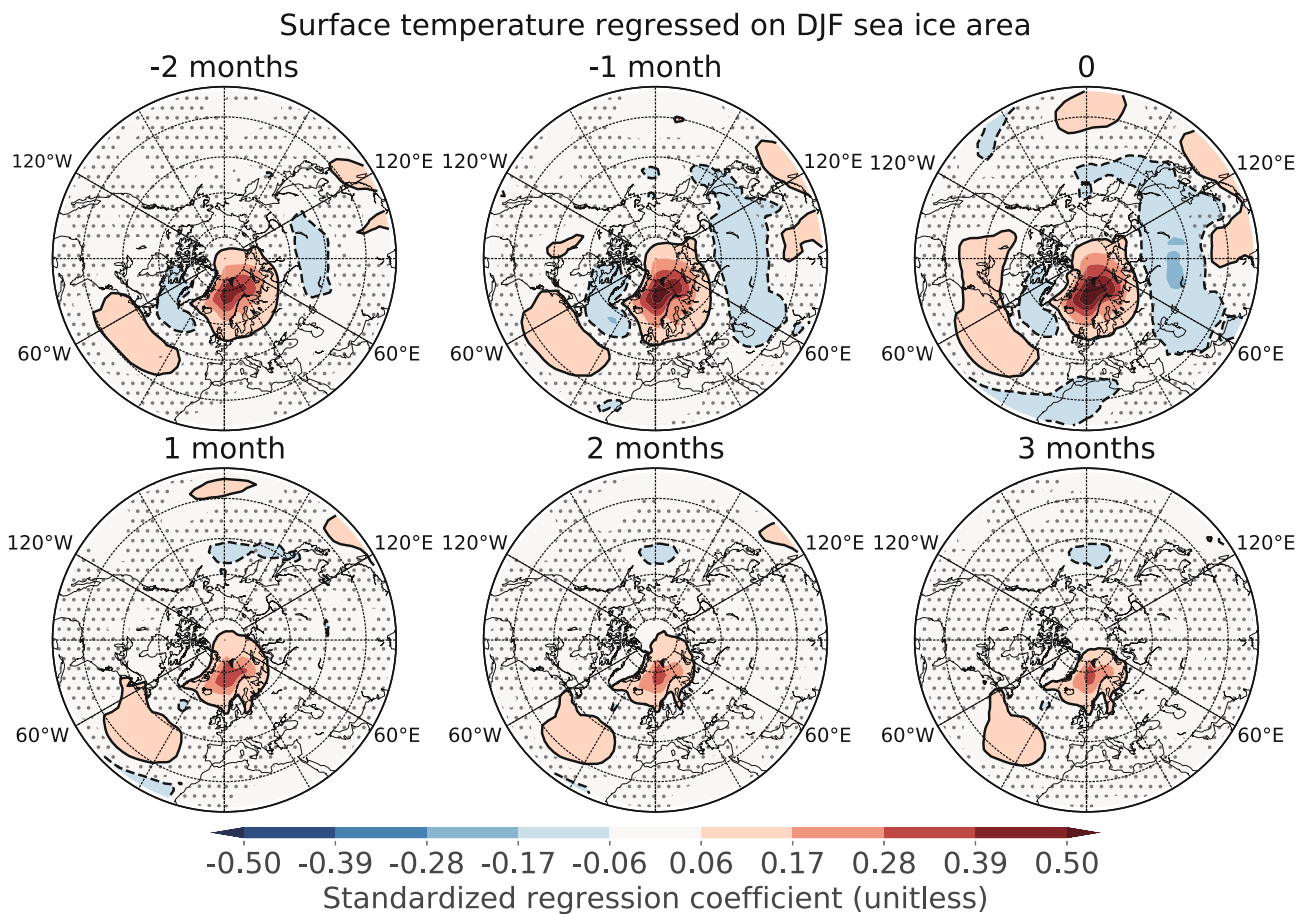
Surface temperature regressed on DJF sea ice area

Fig. 5. Linear regression of winter (DJF) polar cap sea ice area standardized anomalies against standardized surface temperature anomalies between lag −1 months to lead +4 months. The regressions have been multiplied by minus one to show the patterns associated with low sea ice. Blue, dashed contours are cold anomalies; red, solid contours are warm anomalies. The shading is unitless (standardized regression coefficient).

warm Arctic temperatures supports the results presented in the previous section, where warmer midlatitude air is transported to the Arctic, thereby reducing sea ice. The warm anomaly persists over the Barents–Kara Sea at lags of up to 3 months, likely in response to the low sea ice. The cool continental anomaly, however, is only present in the months before low sea ice, and not after. This implies the Eurasian cooling is not a response to low sea ice, but instead is driven by atmospheric circulation changes that precede and contribute to low sea ice. Of note is that we also find no evidence for Eurasian winter cooling following low sea ice in other seasons. More specifically, we find no evidence for Eurasian winter cooling following low autumn sea ice, as suggested by others (e.g., Francis et al., 2009; Hopsch et al., 2012; Jaiser et al., 2012).

3.4.   *Sea level pressure*

To further examine the atmospheric circulation changes linked to the Eurasian cooling, we carry out the same analysis again but with sea level pressure. In the CMIP5 models, the Eurasian cooling is dynamically related to a strengthened Siberian high, consistent with previous studies (Mori et al., 2014; Sun et al., 2016). A high sea level pressure anomaly is

found simultaneously with, and for two months prior to, low winter sea ice, which can be seen in Fig. 6. The strengthened Siberian high appears part of a larger-scale pattern of circulation anomalies, including a positive North Atlantic Oscillation (NAO)-type pattern in the North Atlantic and raised pressure in the North Pacific. The surface circulation anomalies are much weaker at positive lags, with the most notable feature being a negative NAO pattern at lags of 1 and 2 months. There is no evidence of a strengthened Siberian high following low sea ice, which helps explain the lack of Eurasian cooling following low winter sea ice.

Several studies have examined the Siberian winter cooling trend, some of which have found that sea ice loss is a precursor to cold continental temperatures (Petoukhov and Semenov, 2010; Mori et al., 2014). Others, meanwhile, have found that sea ice does not drive the cold continental temperatures, but does force a warming Arctic (McCusker et al., 2016; Sorokina et al., 2016; Sun et al., 2016). Our study falls into the latter category insofar as that, while there is evidence for sea ice loss as a precursor to warmer Arctic surface temperatures, the same cannot be said for cold continental temperatures. Thus far, the causes of the "warm Arctic, cold
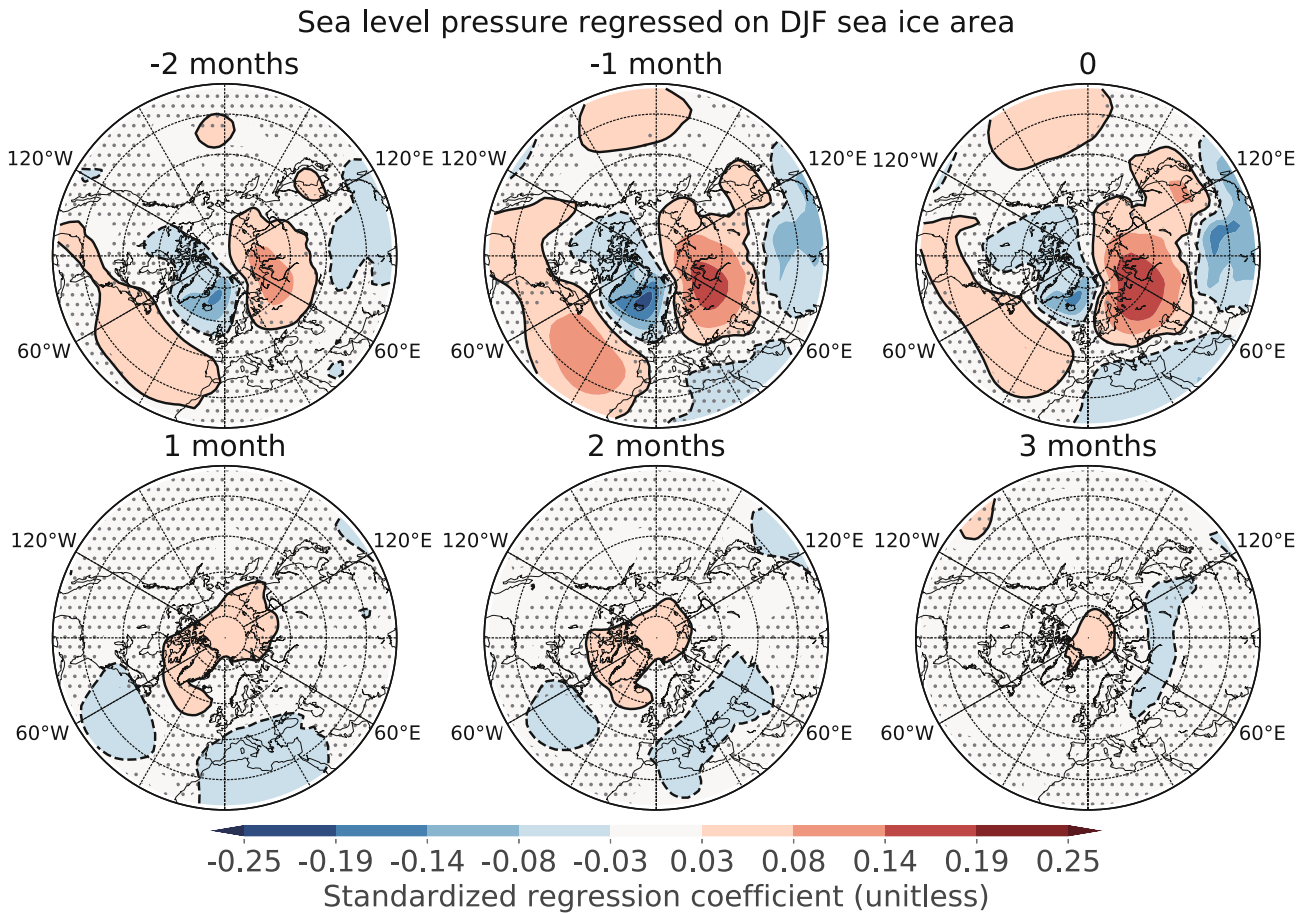
Sea level pressure regressed on DJF sea ice area

Fig. 6. As in Fig. 5 but for standardized mean sea level pressure anomalies. Red, solid contours are high pressure anomalies; blue, dashed contours are low pressure anomalies. The shading is unitless (standardized regression coefficient).

continent" pattern remain uncertain, as discussed in Screen (2017a).

3.5. *Regional sea ice anomalies*

As mentioned earlier, low ice in specific regions of the Arctic can impact the atmosphere in different ways. To examine these relationships, Arctic sea ice is partitioned into the marginal seas shown in Fig. 7, based on those previously used in Screen (2017b). Figures 8 and 9 show regressions of sea ice, averaged over the four selected polar seas, against the polar cap geopotential height and eddy heat flux, respectively. The regressions of Barents–Kara Sea winter sea ice with polar cap height (Fig. 8a) are similar to those previously shown for the pan-Arctic ice area, with positive polar cap height (Fig. 8a) and eddy heat flux (Fig. 9a) anomalies preceding low ice by 2–3 months, and positive polar cap height anomalies following low sea ice. However, in comparison to the regressions with the pan-Arctic sea ice area, the regressions against Barents–Kara Sea ice are weaker at negative lags and strong at positive lags. Broadly similar lead and lag regressions are found for low winter Greenland Sea ice (Figs. 8b and 9b). There are significant (mainly tropospheric) positive polar cap height and eddy heat flux anomalies preceding, and coincident with, low winter Bering Sea ice (Figs. 8c and 9c).

The Sea of Okhotsk has a noticeably distinct pattern from the other seas, with a large negative polar cap height anomaly (Fig. 8d) and negative heat flux (Fig. 9d) in the 2–5 months prior to low ice. This indicates reduced vertical wave activity propagation into the stratosphere and a stronger polar vortex.

4. Conclusions

In this paper, we present a series of regressions of atmospheric variables against Arctic sea ice area at extended leads and lags using output from CMIP5 pre-industrial control simulations. We find statistically significant regressions at both positive and negative lags, suggesting both atmospheric precursors of, and responses to, low sea ice. Despite being robust across models and statistically significant, we note the regressions are fairly modest, suggesting Arctic sea is not the dominant driver of polar-cap-average circulation variability, or vice-versa. Nevertheless, midlatitude circulation anomalies in the form of enhanced meridional eddy heat flux do significantly influence Arctic sea ice area. We find that positive polar cap anomalies, reflecting a weaker polar stratospheric vortex, both precede low sea ice and, in some seasons, also follow low sea ice. Zonal mean meridional eddy heat flux anomalies are shown to be statistically significant prior to low
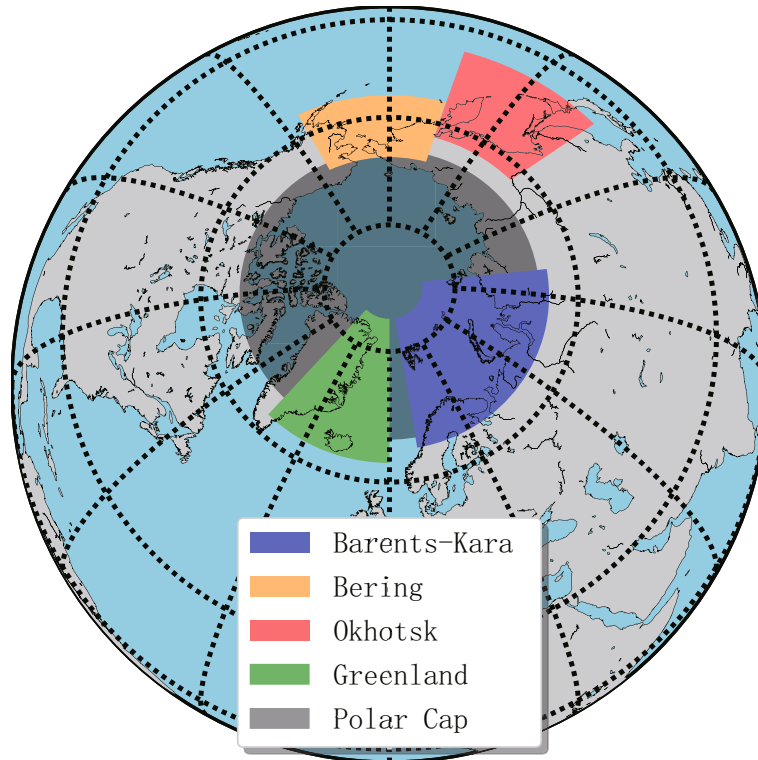
Fig. 7. Geographic regions used for spatial averaging of atmospheric and sea ice variables. Grey is the polar cap; Barents–Kara Sea in blue; Bering Sea in orange; Sea of Okhotsk in red; Greenland Sea in green.
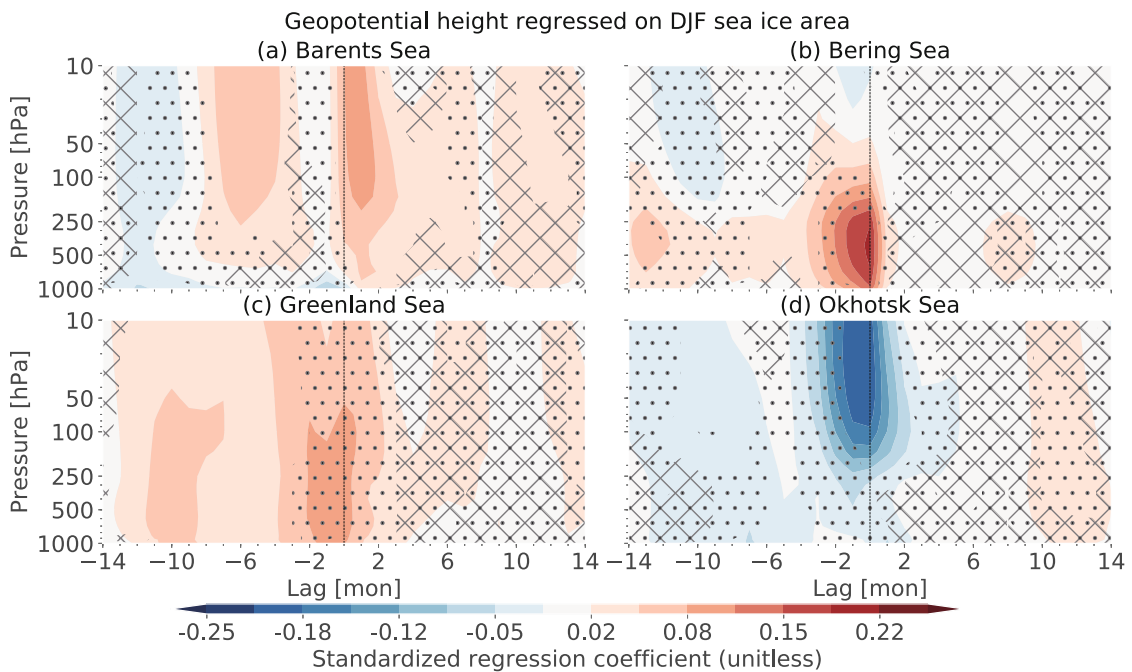

Fig. 8. As in Fig. 2 but for winter (DJF) sea ice standardized anomalies in the (a) Barents–Kara Sea, (b) Bering Sea, (c) Greenland Sea and (d) Sea of Okhotsk.

sea ice, but weaker and not statistically significant following low sea ice. This suggests that midlatitude atmospheric circulation changes, which manifest as an increase in eddy heat flux, lead to changes in Arctic sea ice as well as a weaken-

ing of the polar stratospheric vortex. In this regard, our results provide support for previous studies that have suggested a sizeable component of Arctic mid-tropospheric thickness changes is driven by lower-latitude processes (Screen et al.,
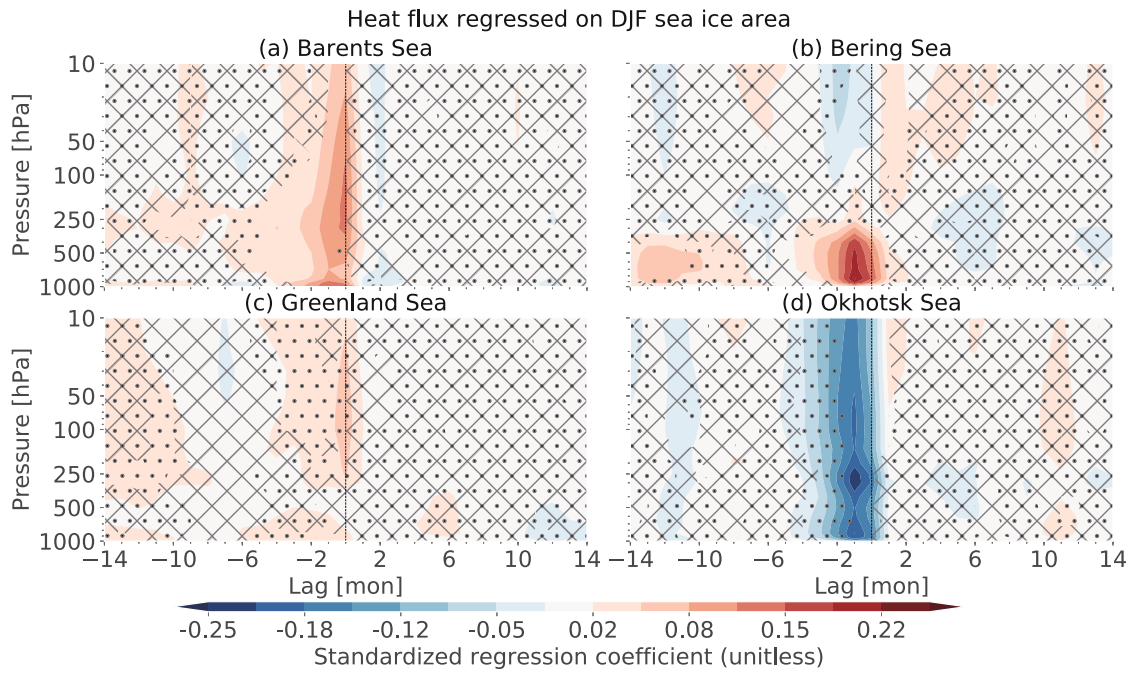
Heat flux regressed on DJF sea ice area

Fig. 9. As in Fig. 8 but for midlatitude meridional eddy heat flux standardized anomalies. The shading is unitless (standardized regression coefficient).

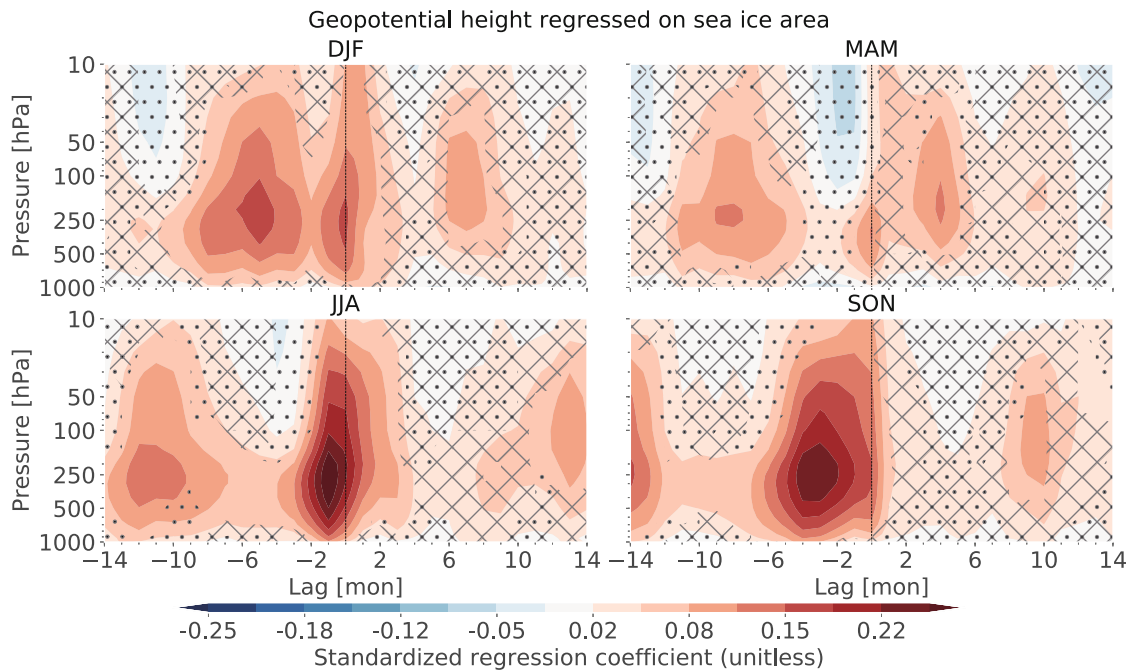Geopotential height regressed on sea ice area

Fig. 10. As in Fig. 2, but for RCP8.5 simulations.

2012; Perlwitz et al., 2015). We argue that whilst low sea ice may enhance Arctic warming and further weaken the polar vortex, it appears that in the first instance both the low sea ice and weakened polar vortex are driven by the enhanced eddy heat flux. This is somewhat different to the conclusions of many studies reviewed by Cohen et al. (2014), which hypothesized that reduced sea ice leads to enhanced wave propaga-

tion from the troposphere to the stratosphere and a weakened polar vortex.

As year-on-year variations in sea ice during the pre-industrial control simulations may be of different magnitude and spatial pattern to those projected in the future, a similar analysis is performed using detrended RCP8.5 projections from the primary subset of models in Table 1. As shown in

Fig. 10, the results are qualitatively similar to those of the pre-industrial control simulations, which further emphasizes the robustness of the results.

We find that low sea ice in winter is associated with warm winter surface temperatures over the Arctic and cold surface temperatures over Eurasia, consistent with previous studies using observations or reanalyses (Cohen et al., 2013; Mori et al., 2014; Kug et al., 2015). The Eurasian cooling is dynamically related to a strengthened Siberian high, again consistent with past work (Mori et al., 2014). Crucially however, we show that both the strengthened Siberian high and the Eurasian cooling are present several months before the low sea ice. In contrast, we find no evidence of a strengthened Siberian high or Eurasian cooling in the months following low winter sea ice. This suggests that the Eurasian cooling is driven by atmospheric circulation anomalies that precede and may contribute to low sea ice, but is not directly driven by low sea ice. This supports the conclusions of Sato et al. (2014), Sorokina et al. (2016), Sun et al. (2016) and McCusker et al. (2016), but is contrary to other studies that proposed a causal relationship between low sea ice and Eurasian cooling (Honda et al., 2009; Petoukhov and Semenov, 2010; Mori et al., 2014; Kug et al., 2015).

Finally, we examine relationships between regional sea ice anomalies and polar cap height. Similar to Sun et al. (2015), we find that low Atlantic sector sea ice, specifically in the Barents–Kara Sea, is correlated with a weakened stratospheric polar vortex; and low Pacific sector sea ice, specifically in the Sea of Okhotsk, is correlated with a strengthened polar vortex. In both cases, the polar cap height anomalies precede low sea ice by several months and are associated with meridional heat flux anomalies that also precede the low sea ice. Thus, our analyses suggest that modified meridional eddy heat flux could contribute simultaneously to both a perturbed polar vortex and low sea ice.

REFERENCES

Baldwin, M. P., and T. J. Dunkerton, 2001: Stratospheric harbingers of anomalous weather regimes. *Science*, **294**, 581–584, https://doi.org/10.1126/science.1063315.

Baldwin, M. P., D. B. Stephenson, D. W. J. Thompson, T. J. Dunkerton, A. J. Charlton, and A. O'Neill, 2003: Stratospheric memory and skill of extended-range weather forecasts. *Science*, **301**, 636–640, https://doi.org/10.1126/science.

1087143.

Boland, E. J. D., T. J. Bracegirdle, and E. F. Shuckburgh, 2017: Assessment of sea ice-atmosphere links in CMIP5 models. *Climate Dyn.*, **49**, 683–702, https://doi.org/10.1007/s00382-016-3367-1.

Christiansen, B., 2001: Downward propagation of zonal mean zonal wind anomalies from the stratosphere to the troposphere: Model and reanalysis. *J. Geophys. Res.*, **106**, 27 307–27 322, https://doi.org/10.1029/2000JD000214.

Cohen, J., J. Jones, J. C. Furtado, and E. Tziperman, 2013: Warm arctic, cold continents: A common pattern related to arctic sea ice melt, snow advance, and extreme winter weather. *Oceanography*, **26**, 150–160, https://doi.org/10.5670/oceanog.2013.70.

Cohen, J., and Coauthors, 2014: Recent arctic amplification and extreme mid-latitude weather. *Nature Geoscience*, **7**, 627–637, https://doi.org/10.1038/ngeo2234.

Edmon, H. J., B. J. Hoskins, and M. E. McIntyre, 1980: Eliassen-palm cross sections for the troposphere. *J. Atmos. Sci.*, **37**, 2600–2616, https://doi.org/10.1175/1520-0469(1980)037<2600:EPCSFT>2.0.CO;2.

Francis, J. A., W. H. Chan, D. J. Leathers, J. R. Miller, and D. E. Veron, 2009: Winter northern hemisphere weather patterns remember summer arctic sea-ice extent. *Geophys. Res. Lett.*, **36**, L07503, https://doi.org/10.1029/2009GL037274.

Garfinkel, C. I., D. L. Hartmann, and F. Sassi, 2010: Tropospheric precursors of anomalous northern hemisphere stratospheric polar vortices. *J. Climate*, **23**, 3282–3299, https://doi.org/10.1175/2010JCLI3010.1.

Honda, M., J. Inoue, and S. Yamane, 2009: Influence of low arctic sea-ice minima on anomalously cold Eurasian winters. *Geophys. Res. Lett.*, **36**, https://doi.org/10.1029/2008GL037079.

Hopsch, S., J. Cohen, and K. Dethloff, 2012: Analysis of a link between fall arctic sea ice concentration and atmospheric patterns in the following winter. *Tellus A*, **64**, 18624, https://doi.org/10.3402/tellusa.v64i0.18624.

Jaiser, R., K. Dethloff, D. Handorf, A. Rinke, and J. Cohen, 2012: Impact of sea ice cover changes on the northern hemisphere atmospheric winter circulation. *Tellus A*, **64**, 11595, https://doi.org/10.3402/tellusa.v64i0.11595.

Kim, B.-M., S.-W. Son, S.-K. Min, J.-H. Jeong, S.-J. Kim, X. D. Zhang, T. Shim, and J.-H. Yoon, 2014: Weakening of the stratospheric polar vortex by arctic sea-ice loss. *Nature Communications*, **5**, 4646, https://doi.org/10.1038/ncomms5646.

Knutti, R., D. Masson, and A. Gettelman, 2013: Climate model genealogy: generation CMIP5 and how we got there. *Geophys. Res. Lett.*, **40**, 1194–1199, https://doi.org/10.1002/grl.50256.

Koenigk, T., M. Caian, G. Nikulin, and S. Schimanke, 2016: Regional arctic sea ice variations as predictor for winter climate conditions. *Climate Dyn.*, **46**, 317–337, https://doi.org/10.1007/s00382-015-2586-1.

Kost, J. T., and M. P. McDermott, 2002: Combining dependent *P*-values. *Statistics & Probability Letters*, **60**, 183–190, https://doi.org/10.1016/S0167-7152(02)00310-3.

Kug, J.-S., J.-H. Jeong, Y.-S. Jang, B.-M. Kim, C. K. Folland, S.-K. Min, and S.-W. Son, 2015: Two distinct influences of arctic warming on cold winters over North America and East Asia. *Nature Geosci*, **8**, 759–762, https://doi.org/10.1038/ngeo2517.

Martius, O., L. M. Polvani, and H. C. Davies, 2009: Blocking precursors to stratospheric sudden warming events. *Geophys. Res. Lett.*, **36**, https://doi.org/10.1029/2009GL038776.

McCusker, K. E., J. C. Fyfe, and M. Sigmond, 2016: Twenty-five winters of unexpected Eurasian cooling unlikely due to arctic sea-ice loss. *Nature Geoscience*, **9**, 838–842, https://doi.org/10.1038/ngeo2820.

Mori, M., M. Watanabe, H. Shiogama, J. Inoue, and M. Kimoto, 2014: Robust arctic sea-ice influence on the frequent Eurasian cold winters in past decades. *Nature Geoscience*, **7**, 869–873, https://doi.org/10.1038/ngeo2277.

Nakamura, T., K. Yamazaki, K. Iwamoto, M. Honda, Y. Miyoshi, Y. Ogawa, Y. Tomikawa, and J. Ukita, 2016: The stratospheric pathway for arctic impacts on midlatitude climate. *Geophys. Res. Lett.*, **43**, 3494–3501, https://doi.org/10.1002/2016GL068330.

Newman, P. A., and E. R. Nash, 2000: Quantifying the wave driving of the stratosphere. *J. Geophys. Res.*, **105**, 12 485–12 497, https://doi.org/10.1029/1999JD901191.

Overland, J. E., and Coauthors, 2016: Nonlinear response of mid-latitude weather to the changing arctic. *Nat. Clim. Change*, **6**, 992–999, https://doi.org/10.1038/nclimate3121.

Pedersen, R. A., I. Cvijanovic, P. L. Langen, and B. M. Vinther, 2016: The impact of regional arctic sea ice loss on atmospheric circulation and the NAO. *J. Climate*, **29**, 889–902, https://doi.org/10.1175/JCLI-D-15-0315.1.

Peings, Y., and G. Magnusdottir, 2014: Response of the wintertime northern hemisphere atmospheric circulation to current and projected arctic sea ice decline: A numerical study with CAM5. *J. Climate*, **27**, 244–264, https://doi.org/10.1175/JCLI-D-13-00272.1.

Perlwitz, J., M. Hoerling, and R. Dole, 2015: Arctic tropospheric warming: Causes and linkages to lower latitudes. *J. Climate*, **28**, 2154–2167, https://doi.org/10.1175/JCLI-D-14-00095.1.

Petoukhov, V., and V. A. Semenov, 2010: A link between reduced Barents-Kara sea ice and cold winter extremes over northern continents. *J. Geophys. Res.*, **115**, https://doi.org/10.1029/2009JD013568.

Sato, K., J. Inoue, and M. Watanabe, 2014: Influence of the gulf stream on the Barents Sea ice retreat and Eurasian cold-ness during early winter. *Environmental Research Letters*, **9**, 084009, https://doi.org/10.1088/1748-9326/9/8/084009.

Screen, J. A., 2017a: Climate science: Far-flung effects of arctic warming. *Nature Geoscience*, **10**, 253–254, https://doi.org/10.1038/ngeo2924.

Screen, J. A., 2017b: Simulated atmospheric response to regional and pan-arctic sea ice loss. *J. Climate*, **30**, 3945–3962, https://doi.org/10.1175/JCLI-D-16-0197.1.

Screen, J. A., C. Deser, and I. Simmonds, 2012: Local and remote controls on observed Arctic warming. *Geophys. Res. Lett.*, **39**, https://doi.org/10.1029/2012GL051598.

Sjoberg, J. P., and T. Birner, 2012: Transient tropospheric forcing of sudden stratospheric warmings. *J. Atmos. Sci.*, **69**, 3420–3432, https://doi.org/10.1175/JAS-D-11-0195.1.

Smith, K. L., P. J. Kushner, and J. Cohen, 2011: The role of linear interference in northern annular mode variability associated with Eurasian snow cover extent. *J. Climate*, **24**, 6185–6202, https://doi.org/10.1175/JCLI-D-11-00055.1.

Sorokina, S. A., C. Li, J. J. Wettstein, and N. G. Kvamst, 2016: Observed atmospheric coupling between Barents Sea ice and the warm-arctic cold-Siberian anomaly pattern. *J. Climate*, **29**, 495–511, https://doi.org/10.1175/JCLI-D-15-0046.1.

Sun, L. T., C. Deser, and R. A. Tomas, 2015: Mechanisms of stratospheric and tropospheric circulation response to projected arctic sea ice loss. *J. Climate*, **28**, 7824–7845, https://doi.org/10.1175/JCLI-D-15-0169.1.

Sun, L., J. Perlwitz, and M. Hoerling, 2016: What caused the recent "warm arctic, cold continents" trend pattern in winter temperatures? *Geophys. Res. Lett.*, **43**, 5345–5352, https://doi.org/10.1002/2016GL069024.

Vihma, T., 2014: Effects of arctic sea ice decline on weather and climate: A review. *Surveys in Geophysics*, **35**, 1175–1214, https://doi.org/10.1007/s10712-014-9284-0.

Walsh, J. E., 2014: Intensified warming of the arctic: Causes and impacts on middle latitudes. *Global and Planetary Change*, **117**, 52–63, https://doi.org/10.1016/j.gloplacha.2014.03.003.